Check for updates

Received: 20 March 2023 | Revised: 19 January 2024 | Accepted: 9 March 2024

DOI: 10.1002/asjc.3385

RESEARCH ARTICLE

WILEY

Observer-based distributed dynamic event-triggered control of multi-agent systems with adjustable interevent time

Zeyuan Wang | **Mohammed Chadli**

University Paris-Saclay, IBISC, Univ Evry, Evry, France

Correspondence
Zeyuan Wang, University Paris-Saclay, IBISC, Univ Evry, 91020 Evry, France.
Email: zeyuan.wang@universite-paris-saclay.fr

Funding information
This research was supported by the China Scholarship Council grant number: 202206020096.

Abstract

In this paper, a novel dynamic event-triggered control protocol for leader-following problems of generic linear multi-agent systems is proposed. Compared with the existing static event-triggered strategy, the developed event-triggered approach significantly reduces the utilization of communication resources while guaranteeing asymptotic consensus, and the interevent time is adjustable. Under this event scheduling mechanism, a synthesis approach combining controller and observer design is presented. The observer-based control and event-triggered rules are distributed, which only require local information of each agent to implement. The proposed methods incorporate model-based estimation and auxiliary dynamic variables with a clock-like behavior to prolong the interevent time as long as possible. The sufficient conditions for leader-following consensus are established using linear matrix inequalities (LMIs) formulation to facilitate numerical computation. Comparative simulations in different scenarios demonstrate the validity of the proposed theoretical results.

KEYWORDS

distributed control, dynamic event-triggered control, leader-following consensus, multi-agent systems, observer-based control

1 | INTRODUCTION

The research of multi-agent systems (MASs) originated in the 1980s and experienced rapid growth in the mid-1990s. In recent years, the development of technologies such as unmanned aerial vehicle coordination, underwater cooperation, and robot formation control has brought consensus issues in MASs to the forefront of research. One of the particularly intriguing topics is leader-following consensus, also known as model reference consensus [1], where a group of agents need to achieve consensus with the leader agents. This topic has been extensively explored for both linear [2] and nonlinear MASs [3] and for MASs comprising homogeneous or heterogeneous agents [4], and the techniques used for leader-following consensus can be extended to formation control such as in Antonio et al. [5]. Different constraints has also been investigated, such as the presence of faults [6, 7], noise [8], time-varying delay [9], cyberattacks [10], and switching topology [11]. A more detailed survey of recent advance in MASs could be found in Amirkhani and Barshooi [12].

In a time-triggered control system, control updates and data transmissions occur on a periodic schedule. This can lead to an excessive burden for MASs on communication networks as well as an increase in computing resources [13]. This problem motivated an event-triggered mechanism (ETM), which enables a minimum rate of data sampling, communication, and control update while

© 2024 Chinese Automatic Control Society and John Wiley & Sons Australia, Ltd

still ensuring system performance. ETMs for stabilization control are first introduced in Tabuada [14], then gain significant development, and are applied in different dynamic systems [15]. After ETMs were applied to handle the leaderless consensus problem of MASs in Dimarogonas et al. [16], it has been developed for second-order linear MASs [17], generic linear MASs [18] and nonlinear MASs [19]. Recently, many researchers have also developed ETM-based distributed protocols. In Li et al. [20], an adaptive fully distributed event-triggered/self-triggered control is proposed. To address the challenge of unknown input from the leader, an edge-based distributed ETM is proposed in Cheng and Li [21] for coordinated tracking problems. In Xu et al. [22], an observer-based fully ETM protocol is proposed, introducing two novel event-triggered schemes. However, it still remains a challenge for the aforementioned studies to flexibly tune the interevent time as required. A more comprehensive survey of ETMs for MASs could be found in Nowzari et al. [23].

Based on ETMs, a dynamic event-triggered mechanism (DETM) was proposed to increase the interevent time with a more flexible parameter tuning approach [24]. By introducing auxiliary dynamic variables (ADVs), the additional dynamic results in a more intelligent event-triggering decision, enabling a lower sampling rate while still keeping the performance [25]. In He et al. [26], a distributed dynamic event-triggered strategy is first proposed for generic linear MASs, where the event threshold is dynamically changing with the aide of the auxiliary variables. In Hou and Dong [27], a robust DETM is proposed subject to disturbance with guaranteed performance. Additionally, Hou and Dong [28] propose a robust adaptive DETM to address challenges related to actuator faults and external disturbance. Notably, in Berneburg and Nowzari [29] and Wu et al. [30], the proposed clock-like ADVs give more freedom to select a preferred (minimum) interevent time by choosing appropriate parameters in the controller design phase, and the Zeno behavior of MAS is excluded. Similar idea has also been explored in Wang and Chadli [31] for directed topology. In Wang and Chadli [32], an improved DETM is proposed with a moving average method under a centralized control scheme.

Most existing event-triggered control methods for MASs assume that all states of agents are available. This assumption is not always valid in reality because the existence of nonmeasurable state. Observers are required to estimate the system's internal states. Indeed, in Zhang et al. [33], the control/observer co-design problem for generic linear MASs in the leaderless consensus scenario is studied. The results are then developed in Hu et al. [34] for the leader-following problem but only apply to second-order linear MASs. A more generic approach is proposed in Trejo et al. [6], which uses LMIs to synthesize the controller and observer, but the final strategy is not distributed. There is only few literature utilizing DETM. Noticeably, literature in earlier studies [35, 36] designs observers-based DETMs and eliminates the Zeno behavior, but the complexity of parameter tuning presents a challenge in designing the minimum interevent time (MIET) quantitatively. Based on the above discussion, the synthesis of a distributed controller and observer under DETM with adjustable MIET has yet to be fully explored.

This work is inspired by Berneburg and Nowzari [29, 30], where DETMs are realized based on clock-like ADVs to facilitate the MIET adjustment. However, in Wu et al. [30], a bad ADV will fail to achieve leader-following consensus because of a discontinuous Lyapunov function chosen. The proposed DETM only guarantees stability between two consecutive events but not globally, though the authors omitted this critical remark. Based on the above discussion, the DETM in Wu et al. [30] is improved, and a novel controller/observer synthesis method using the bilinear matrix inequality ($\mathcal{BMI}$) and $\mathcal{LMI}$ approach is proposed. The main contributions of this paper are summarized as follows.

1. The study proposes a distributed, dynamic event-triggered control for addressing leader-following problems using clock-like auxiliary variables. This mechanism reduces the communication frequency while ensuring asymptotic convergence of the system. By tuning the upper bound of the auxiliary variables, the interevent time can be adjusted as required without the risk of Zeno behavior. Compared with the existing research [30, 33–36], the proposed method enables a more flexible tuning of interevent time for generic linear MASs with limited information availability.
2. Compared with Trejo et al. [6], the observer-based controller and event-triggered rule designed for each agent are distributed and require only local information for implementation. Moreover, compared with prior research [6, 18,37], the proposed feedback control law adopts model-based combinatory measurement error, which grows slower than the trivial model-free measurement, enabling a longer interevent time.
3. Novel criteria for determining the gain of controllers and observers under the proposed DETM are established using $\mathcal{LMI}s$ in order to facilitate numerical computation.

The rest of the paper is structured as follows: In Section 2, preliminaries, including notations and graph theory, are provided. Section 3 presents the problem formulation and assumptions. The proposed distributed control protocol for leader-following control is detailed in Section 4. The effectiveness of the proposed strategies through numerical simulations is demonstrated in Section 5.

19346093, 0, Downloaded from https://onlinelibrary.wiley.com/doi/10.1002/asjc.3385 by Universite Paris-Saclay, Wiley Online Library on [29/04/2024]. See the Terms and Conditions (https://onlinelibrary.wiley.com/terms-and-conditions) on Wiley Online Library for rules of use; OA articles are governed by the applicable Creative Commons License

2 | PRELIMINARIES

Let $\mathbb{R}$ denote the set of real numbers. Given a matrix $\boldsymbol{S}$, $\boldsymbol{S}^T$ denotes its transpose. If $\boldsymbol{S}$ is a square matrix, $\lambda_{\min}(\boldsymbol{S})$ and $\lambda_{\max}(\boldsymbol{S})$ denote the minimum and maximum eigenvalues of $\boldsymbol{S}$, respectively, and $\boldsymbol{S}^{-1}$ represents its inverse. For a symmetric matrix $\boldsymbol{S}, \boldsymbol{S} > 0$ (resp. $S \geq 0$) denotes that $\boldsymbol{S}$ is positive definite (resp. positive semidefinite), and $\boldsymbol{S} < 0$ (resp. $S \leq 0$) means $-\boldsymbol{S} > 0$ (resp. $-S \geq 0$). $\boldsymbol{I}_n$ (resp. $\boldsymbol{I}$) denotes an identity matrix of dimension n (resp. of appropriate dimension). $\boldsymbol{0}_{m\times n}$ denotes a zero matrix of dimension $m \times n$. $\otimes$ denotes the Kronecker product. $\|\cdot\|$ denotes ℓ_2-norm for vectors or spectrum norm for matrices. Let $*$ denote the symmetric entries in a matrix. Let $S = \operatorname{diag}(s_1, \dots, s_N)$ denote an $N \times N$ diagonal matrix whose entries are $s_1, s_2, \dots, s_N$.

The communication topology of N follower agents is represented by an undirected weighted graph $\mathcal{G} = (\mathcal{V}, \mathcal{E})$ consisting of a vertex set $\mathcal{V} = \{v_1, \dots, v_N\}$ and an edge set $\mathcal{E} \subseteq \mathcal{V} \times \mathcal{V}$. Follower agent i and the leader are represented as vertices v_i and v_0, respectively. Denote $\mathcal{N}_i$ the set of neighbors of agent i. The weighted adjacency matrix $\mathcal{A} = (a_{ij}) \in \mathbb{R}^{N\times N}$ of $\mathcal{G}$ is defined such that $a_{ii} = 0$, $a_{ij} > 0$ if v_i is connected to v_j and $a_{ij} = 0$ otherwise. The Laplacian matrix $\mathcal{L} = (l_{ij}) \in \mathbb{R}^{N\times N}$ is defined as $l_{ii} = \sum_{j=1,j\neq i}^{N} a_{ij}$ and $l_{ij} = -a_{ij}, i \neq j$. Define $\bar{\mathcal{G}} = (\bar{\mathcal{V}}, \bar{\mathcal{E}})$ the augmented graph of $\mathcal{G}$, with $\bar{\mathcal{V}} = \mathcal{V} \cup \{v_0\}$ and $(v_i, v_0) \in \bar{\mathcal{E}}$ if agent i is connected to the leader. Define leader adjacency matrix $\mathcal{D} = \operatorname{diag}(d_1, \dots, d_N)$ as a diagonal matrix where its diagonal element $d_i > 0$ if $(v_i, v_0) \in \bar{\mathcal{E}}$ otherwise $d_i = 0$. Define $\mathcal{H} = \mathcal{L} + \mathcal{D}$.

3 | PROBLEM STATEMENT

Consider a linear MAS with N follower agents and one leader represented by

$$\begin{cases} \dot{\boldsymbol{x}}_i(t) &= \boldsymbol{A}\boldsymbol{x}_i(t) + \boldsymbol{B}\boldsymbol{u}_i(t), i = 1, \dots, N \\ \boldsymbol{y}_i(t) &= \boldsymbol{C}\boldsymbol{x}_i(t), i = 1, \dots, N \\ \dot{\boldsymbol{x}}_0(t) &= \boldsymbol{A}\boldsymbol{x}_0(t) \end{cases} \tag{1}$$

where $\boldsymbol{x}_i(t)$ and $\boldsymbol{x}_0(t)$ denote the states of follower agents and the leader, respectively. $\boldsymbol{y}_i(t)$ is the output of agent i, $\boldsymbol{u}_i(t) \in \mathbb{R}^m$ is the control input of agent i. $\boldsymbol{A} \in \mathbb{R}^{n\times n}, \boldsymbol{B} \in \mathbb{R}^{n\times m}$, $\boldsymbol{C} \in \mathbb{R}^{r\times n}$. Define the consensus error of agent i as $\xi_i(t) = \boldsymbol{x}_i(t) - \boldsymbol{x}_0(t)$ and $\xi(t) = \left[\xi_1^T(t), \dots, \xi_N^T(t)\right]^T$. The objective of this study is to design an event-based control law such that all follower agents and the leader achieve the consensus, that is,

$$\lim_{t\to\infty} \|\xi_i(t)\| = 0, \ \forall i \in \{1, \dots, N\} \tag{2}$$

In order to estimate the internal agents' internal states, Luenberger-type observers are designed for each follower agent i to reconstruct the state $\boldsymbol{x}_i(t)$ from the output $\boldsymbol{y}_i(t)$ and the input $\boldsymbol{u}_i(t)$:

$$\begin{cases} \dot{\tilde{\boldsymbol{x}}}_i(t) = \boldsymbol{A}\tilde{\boldsymbol{x}}_i(t) + \boldsymbol{B}\boldsymbol{u}_i(t) + \boldsymbol{L}_o(\tilde{\boldsymbol{y}}_i(t) - \boldsymbol{y}_i(t)) \\ \tilde{\boldsymbol{y}}_i(t) = \boldsymbol{C}\tilde{\boldsymbol{x}}_i(t) \end{cases} \tag{3}$$

where $\boldsymbol{L}_o \in \mathbb{R}^{n\times r}$ and $\tilde{\boldsymbol{x}}_i(t)$ is the observer state. Define observer error of agent i as $\zeta_i(t) = \tilde{\boldsymbol{x}}_i(t) - \boldsymbol{x}_i(t)$ and $\zeta(t) = \left[\zeta_1^T(t), \dots, \zeta_N^T(t)\right]^T$. The proposed event-triggered control input $\boldsymbol{u}_i(t)$ of agent i is defined as

$$\begin{cases} \boldsymbol{u}_i(t) = \boldsymbol{K}\boldsymbol{z}_i(t) \\ \boldsymbol{z}_i(t) = \sum\limits_{j\in\mathcal{N}_i} a_{ij}(\hat{\boldsymbol{x}}_j(t) - \hat{\boldsymbol{x}}_i(t)) + d_i(\boldsymbol{x}_0(t) - \hat{\boldsymbol{x}}_i(t)) \end{cases} \tag{4}$$

where $\boldsymbol{K} \in \mathbb{R}^{m\times n}$ is the gain of the feedback control. $\boldsymbol{z}_i(t)$ is the combinatory state. Define $\boldsymbol{z}(t) = [\boldsymbol{z}_1^T(t), \dots, \boldsymbol{z}_N^T(t)]^T$. $\hat{\boldsymbol{x}}_i(t), i \in \{1, \dots, N\}$ is defined as follows:

$$\hat{\boldsymbol{x}}_i(t) = \tilde{\boldsymbol{x}}_i\left(t_k^i\right) e^{\boldsymbol{A}(t-t_k^i)}, \ t \in \left[t_k^i, t_{k+1}^i\right) \tag{5}$$

where $\tilde{\boldsymbol{x}}_i(t_k^i)$ is the observer state at the last triggering moment t_k^i and t_{k+1}^i is defined by event-triggered rules given in following sections. Define measurement error of agent i as $\boldsymbol{e}_i(t) = \hat{\boldsymbol{x}}_i(t) - \tilde{\boldsymbol{x}}_i(t)$ and $\boldsymbol{e}(t) = \left[\boldsymbol{e}_1^T(t), \dots, \boldsymbol{e}_N^T(t)\right]^T$.

Remark 1. The term $\hat{\boldsymbol{x}}_i(t) = \tilde{\boldsymbol{x}}_i(t_k^i)e^{\boldsymbol{A}(t-t_k^i)}$ is a kind of model-based estimation [38]. Since the trivial estimation $\hat{\boldsymbol{x}}_i(t) = \tilde{\boldsymbol{x}}_i(t_k^i)$ may differ from $\tilde{\boldsymbol{x}}_i(t)$ very quickly, the exponential term $e^{\boldsymbol{A}}$ with agent's dynamic matrix $\boldsymbol{A}$ is used to reduce the error between $\hat{\boldsymbol{x}}_i(t)$ and $\tilde{\boldsymbol{x}}_i(t)$ thus usually increases the interevent time.

By definition of $\xi_i(t)$, $\zeta_i(t)$ and $\boldsymbol{e}_i(t)$, one can deduce $\boldsymbol{z}_i(t)$ as

$$\boldsymbol{z}_i(t) = \sum_{j\in\mathcal{N}_i} a_{ij}(\boldsymbol{e}_j - \boldsymbol{e}_i + \zeta_j - \zeta_i + \xi_j - \xi_i) + d_i(-\boldsymbol{e}_i - \zeta_i - \xi_i) \tag{6}$$

then one can have $\boldsymbol{z} = -(\mathcal{H}\otimes\boldsymbol{I}_n)(\boldsymbol{e}+\zeta+\xi)$ and the following expressions:

$$\begin{cases} \dot{\xi} = (\boldsymbol{I}_N \otimes \boldsymbol{A} - \mathcal{H} \otimes \boldsymbol{BK})\xi - (\mathcal{H} \otimes \boldsymbol{BK})(\zeta + \boldsymbol{e}) \\ \dot{\zeta} = (\boldsymbol{I}_N \otimes (\boldsymbol{A} + \boldsymbol{L}_o\boldsymbol{C}))\zeta \\ \dot{\boldsymbol{e}} = (\mathcal{H} \otimes \boldsymbol{BK})\xi + (\boldsymbol{I}_N \otimes \boldsymbol{A} + \mathcal{H} \otimes \boldsymbol{BK})\boldsymbol{e} \\ \quad + (\mathcal{H} \otimes \boldsymbol{BK} - \boldsymbol{I}_N \otimes \boldsymbol{L}_o\boldsymbol{C})\zeta \end{cases} \tag{7}$$

The following assumptions hold in this paper:

Assumption 1. The pair $(\boldsymbol{A}, \boldsymbol{B})$ is stabilizable and the pair $(\boldsymbol{A}, \boldsymbol{C})$ is observable.

Assumption 2. The augmented graph $\bar{\mathcal{G}}$ is fixed and undirected and contains a spanning tree with the leader agent being its root.

19346093, 0, Downloaded from https://onlinelibrary.wiley.com/doi/10.1002/asjc.3385 by Universite Paris-Saclay, Wiley Online Library on [29/04/2024]. See the Terms and Conditions (https://onlinelibrary.wiley.com/terms-and-conditions) on Wiley Online Library for rules of use; OA articles are governed by the applicable Creative Commons License

4 | MAIN RESULTS

This section presents a comprehensive controller and observer design for the leader-following consensus control under the DETM strategy.

4.1 | Observer and controller synthesis

This section presents a distributed design of controllers and observers for follower agents and the DETM rule to determine the nonperiodic data transmission protocol.

Theorem 1. *Suppose that the assumptions in Section 3 are all satisfied. The MAS described in (1) will achieve leader-following consensus if the following $\mathcal{BMI}s$ are satisfied with regard to $\boldsymbol{P}_1 > 0, \boldsymbol{P}_2 > 0$, the controller gain $\boldsymbol{K}$, and the observer gain $\boldsymbol{L}_o$:*

$$\boldsymbol{S} = \begin{pmatrix} \boldsymbol{S}_{11} & \boldsymbol{S}_{12} \\ * & \boldsymbol{S}_{22} \end{pmatrix} < 0 \tag{8}$$

where $\boldsymbol{S}_{11}$, $\boldsymbol{S}_{12}$, and $\boldsymbol{S}_{22}$ are defined as

$$\begin{cases} \boldsymbol{S}_{11} = \boldsymbol{I}_N \otimes (\boldsymbol{P}_1\boldsymbol{A} + \boldsymbol{A}^T\boldsymbol{P}_1) - \mathcal{H} \otimes (\boldsymbol{P}_1\boldsymbol{B}\boldsymbol{K} + \boldsymbol{K}^T\boldsymbol{B}^T\boldsymbol{P}_1) \\ \boldsymbol{S}_{12} = -\mathcal{H} \otimes (\boldsymbol{P}_1\boldsymbol{B}\boldsymbol{K}) \\ \boldsymbol{S}_{22} = \boldsymbol{I}_N \otimes (\boldsymbol{P}_2\boldsymbol{A} + \boldsymbol{A}^T\boldsymbol{P}_2 + \boldsymbol{P}_2\boldsymbol{L}_o\boldsymbol{C} + \boldsymbol{C}^T\boldsymbol{L}_o^T\boldsymbol{P}_2) \\ \qquad + (b_1 + b_2)\boldsymbol{I}_{Nn} \end{cases} \tag{9}$$

with any $b_1, b_2 > 0$. And the event-triggered rule of agent i is defined as

$$\begin{aligned} & t_{k+1}^i \triangleq \inf\left\{t > t_k^i | \theta_i(t) \le 0\right\}, \theta_i(t_k^i) = \bar{\theta}_i \\ & \dot{\theta}_i(t) = \begin{cases} \min(\omega_i(t), 0) - \tau_i & \text{if } \|\boldsymbol{e}_i(t)\| \ne 0 \\ -\tau_i & \text{otherwise} \end{cases}, t \in \left[t_k^i, t_{k+1}^i\right) \end{aligned} \tag{10}$$

where $\bar{\theta}_i$ and τ_i are arbitrary positive constants and $\omega_i(t)$ is defined as follows:

$$\begin{aligned} \omega_i(t) \triangleq & -\frac{\boldsymbol{e}_i^T\boldsymbol{Q}\boldsymbol{e}_i}{\boldsymbol{e}_i^T\boldsymbol{P}_3\boldsymbol{e}_i} - \frac{\epsilon\left(\frac{1}{k} - \frac{1}{2\delta_{\max}^2}\right)}{\boldsymbol{e}_i^T\boldsymbol{P}_3\boldsymbol{e}_i}\|\boldsymbol{z}_i\|^2 \\ & - \frac{\boldsymbol{e}_i^T(2\boldsymbol{M}_1 - 2\theta_i\boldsymbol{M}_3)\boldsymbol{z}_i}{\boldsymbol{e}_i^T\boldsymbol{P}_3\boldsymbol{e}_i} \end{aligned} \tag{11}$$

where

$$\begin{cases} \boldsymbol{Q} = \left(\frac{\epsilon k}{\delta_{\min}^2} - \frac{\epsilon}{2} + 2\delta_{\max}\|\boldsymbol{M}_1\|\right)\boldsymbol{I}_n + 2\theta_i\boldsymbol{P}_3\boldsymbol{A} \\ \qquad + \frac{\delta_{\max}^2}{b_1}\boldsymbol{M}_1^T\boldsymbol{M}_1 + \frac{\theta_i^2}{b_2}\boldsymbol{M}_2^T\boldsymbol{M}_2 \\ \boldsymbol{M}_1 = \boldsymbol{K}^T\boldsymbol{B}^T\boldsymbol{P}_1, \boldsymbol{M}_2 = \boldsymbol{P}_3\boldsymbol{L}_o\boldsymbol{C}, \boldsymbol{M}_3 = \boldsymbol{P}_3\boldsymbol{B}\boldsymbol{K} \end{cases} \tag{12}$$

and $\delta_{\min} = \lambda_{\min}(\mathcal{H})$, $\delta_{\max} = \lambda_{\max}(\mathcal{H})$, $k > 2\delta_{\max}^2$, $\boldsymbol{P}_3 > 0$. ϵ is a positive scalar satisfying $\boldsymbol{S} + \epsilon\boldsymbol{I} \le 0$.

Proof. The proof consists of showing the stability of the closed-loop system (7) by Lyapunov theorem. Choose the following Lyapunov function $V(t) = V_1(t) + V_2(t) + V_3(t)$:

$$\begin{cases} V_1(t) = \xi(t)^T(\boldsymbol{I}_N \otimes \boldsymbol{P}_1)\xi(t) \\ V_2(t) = \boldsymbol{\zeta}(t)^T(\boldsymbol{I}_N \otimes \boldsymbol{P}_2)\boldsymbol{\zeta}(t) \\ V_3(t) = \boldsymbol{e}(t)^T(\boldsymbol{\Theta}(t) \otimes \boldsymbol{P}_3)\boldsymbol{e}(t) \end{cases} \tag{13}$$

where $\boldsymbol{P}_1, \boldsymbol{P}_2, \boldsymbol{P}_3 > 0$, $\boldsymbol{\Theta}(t) = \mathrm{diag}(\theta_1(t), \dots, \theta_N(t)) > 0$, and $\dot{\boldsymbol{\Theta}}(t) < 0$ by definition of event-triggered rule (10); thus, $V(t) \ge 0$. The derivatives of V_1, V_2, V_3 along the system trajectory are

$$\begin{cases} \dot{V}_1 = 2\xi^T(\boldsymbol{I}_N \otimes \boldsymbol{P}_1\boldsymbol{A} - \mathcal{H} \otimes \boldsymbol{M}_1^T)\xi \\ \qquad - 2\xi^T(\mathcal{H} \otimes \boldsymbol{M}_1^T)\boldsymbol{e} - 2\xi^T(\mathcal{H} \otimes \boldsymbol{M}_1^T)\boldsymbol{\zeta} \\ \dot{V}_2 = 2\boldsymbol{\zeta}^T(\boldsymbol{I}_N \otimes \boldsymbol{P}_2(\boldsymbol{A} + \boldsymbol{L}_o\boldsymbol{C}))\boldsymbol{\zeta} \\ \dot{V}_3 = 2\boldsymbol{e}^T(\boldsymbol{\Theta} \otimes \boldsymbol{P}_3\boldsymbol{A} + \boldsymbol{\Theta}\mathcal{H} \otimes \boldsymbol{M}_3)\boldsymbol{e} \\ \qquad + 2\boldsymbol{e}^T(\boldsymbol{\Theta}\mathcal{H} \otimes \boldsymbol{M}_3)\xi + \boldsymbol{e}^T(\dot{\boldsymbol{\Theta}} \otimes \boldsymbol{P}_3)\boldsymbol{e} \\ \qquad + 2\boldsymbol{e}^T(\boldsymbol{\Theta}\mathcal{H} \otimes \boldsymbol{M}_3 - \boldsymbol{\Theta} \otimes \boldsymbol{M}_2)\boldsymbol{\zeta} \end{cases} \tag{14}$$

Notice that under Assumption 2, the matrix $\mathcal{H}$ is positive definite and invertible. By using the fact that $\boldsymbol{\xi} = -(\mathcal{H}^{-1} \otimes \boldsymbol{I})\boldsymbol{z} - \boldsymbol{e} - \boldsymbol{\zeta}$ and (14) to calculate $\dot{V}(t)$, one can obtain

$$\begin{aligned} \dot{V} &= \dot{V}_1 + \dot{V}_2 + \dot{V}_3 \\ &= 2\xi^T(\boldsymbol{I}_N \otimes \boldsymbol{P}_1\boldsymbol{A} - \mathcal{H} \otimes \boldsymbol{M}_1^T)\xi - 2\xi^T(\mathcal{H} \otimes \boldsymbol{M}_1^T)\boldsymbol{\zeta} \\ &\quad + 2\boldsymbol{\zeta}^T(\boldsymbol{I}_N \otimes \boldsymbol{P}_2(\boldsymbol{A} + \boldsymbol{L}_o\boldsymbol{C}))\boldsymbol{\zeta} \\ &\quad + 2\boldsymbol{e}^T(\mathcal{H} \otimes \boldsymbol{M}_1 - \boldsymbol{\Theta} \otimes \boldsymbol{M}_2)\boldsymbol{\zeta} \\ &\quad - 2\boldsymbol{e}^T(\boldsymbol{\Theta} \otimes \boldsymbol{M}_3 - \boldsymbol{I}_N \otimes \boldsymbol{M}_1)\boldsymbol{z} \\ &\quad + 2\boldsymbol{e}^T(\boldsymbol{\Theta} \otimes \boldsymbol{P}_3\boldsymbol{A} + \mathcal{H} \otimes \boldsymbol{M}_1)\boldsymbol{e} + \boldsymbol{e}^T(\dot{\boldsymbol{\Theta}} \otimes \boldsymbol{P}_3)\boldsymbol{e} \end{aligned} \tag{15}$$

Using Cauchy–Schwarz inequality, one can get

$$\begin{aligned} & 2\boldsymbol{e}^T(\mathcal{H} \otimes \boldsymbol{M}_1 - \boldsymbol{\Theta} \otimes \boldsymbol{M}_2)\boldsymbol{\zeta} \\ & \le \frac{1}{b_1}\boldsymbol{e}^T(\mathcal{H}^2 \otimes \boldsymbol{M}_1^T\boldsymbol{M}_1)\boldsymbol{e} + \frac{1}{b_2}\boldsymbol{e}^T(\boldsymbol{\Theta}^2 \otimes \boldsymbol{M}_2^T\boldsymbol{M}_2)\boldsymbol{e} \\ & \quad + (b_1 + b_2)\boldsymbol{\zeta}^T\boldsymbol{\zeta}, \ b_1, b_2 > 0 \end{aligned} \tag{16}$$

then

$$\begin{aligned} \dot{V} &= 2\xi^T(\boldsymbol{I}_N \otimes \boldsymbol{P}_1\boldsymbol{A} - \mathcal{H} \otimes \boldsymbol{M}_1^T)\xi - 2\xi^T(\mathcal{H} \otimes \boldsymbol{M}_1^T)\boldsymbol{\zeta} \\ &\quad + 2\boldsymbol{\zeta}^T(\boldsymbol{I}_N \otimes \boldsymbol{P}_2(\boldsymbol{A} + \boldsymbol{L}_o\boldsymbol{C}))\boldsymbol{\zeta} + (b_1 + b_2)\boldsymbol{\zeta}^T\boldsymbol{\zeta} \\ &\quad + \boldsymbol{e}^T\left(\frac{\mathcal{H}^2}{b_1} \otimes \boldsymbol{M}_1^T\boldsymbol{M}_1 + \frac{\boldsymbol{\Theta}^2}{b_2} \otimes \boldsymbol{M}_2^T\boldsymbol{M}_2\right)\boldsymbol{e} \\ &\quad - 2\boldsymbol{e}^T(\boldsymbol{\Theta} \otimes \boldsymbol{M}_3 - \boldsymbol{I}_N \otimes \boldsymbol{M}_1)\boldsymbol{z} \\ &\quad + 2\boldsymbol{e}^T(\boldsymbol{\Theta} \otimes \boldsymbol{P}_3\boldsymbol{A} + \mathcal{H} \otimes \boldsymbol{M}_1)\boldsymbol{e} + \boldsymbol{e}^T(\dot{\boldsymbol{\Theta}} \otimes \boldsymbol{P}_3)\boldsymbol{e} \end{aligned} \tag{17}$$

Since the internal state variables $\boldsymbol{\xi}$ and $\boldsymbol{\zeta}$ are not available in control implementation, the idea is to guarantee $\dot{V}$ always negative with arbitrary ξ and $\boldsymbol{\zeta}$. Notice that the first four terms in (17): $2\boldsymbol{\xi}^T(\boldsymbol{I}_N \otimes \boldsymbol{P}_1\boldsymbol{A} - \mathcal{H} \otimes \boldsymbol{M}_1^T)\xi - 2\xi^T(\mathcal{H} \otimes \boldsymbol{M}_1^T)\boldsymbol{\zeta} + 2\boldsymbol{\zeta}^T(\boldsymbol{I}_N \otimes \boldsymbol{P}_2(\boldsymbol{A} + \boldsymbol{L}_o\boldsymbol{C}))\boldsymbol{\zeta} + (b_1 + b_2)\boldsymbol{\zeta}^T\boldsymbol{\zeta}$ form a quadratic expression with regard to $\boldsymbol{\xi}$ and $\boldsymbol{\zeta}$, which could be written as $\boldsymbol{\delta}^T\boldsymbol{S}\boldsymbol{\delta}$, with

19346093, 0, Downloaded from https://onlinelibrary.wiley.com/doi/10.1002/asjc.3385 by Universite Paris-Saclay, Wiley Online Library on [29/04/2024]. See the Terms and Conditions (https://onlinelibrary.wiley.com/terms-and-conditions) on Wiley Online Library for rules of use; OA articles are governed by the applicable Creative Commons License

$$\boldsymbol{\delta} = \begin{pmatrix} \xi \\ \zeta \end{pmatrix} \text{ and } \boldsymbol{S} \text{ defined in (8).} \tag{18}$$

Since $\boldsymbol{S} < 0$ and $\boldsymbol{S} + \epsilon \boldsymbol{I} \leq 0$, one can have $\boldsymbol{\delta}^T \boldsymbol{S} \boldsymbol{\delta} \leq -\epsilon \|\boldsymbol{\delta}\|^2 = -\epsilon(\|\xi\|^2 + \|\zeta\|^2)$. And notice that

$$-\epsilon(\|\xi\|^2 + \|\zeta\|^2) \leq -\epsilon \frac{(\xi+\zeta)^T(\xi+\zeta)}{2} \tag{19}$$

For the sake of brevity, let $\mathcal{H}^{-2}$ denote $\left(\mathcal{H}^{-1}\right)^2$. Substituting $\boldsymbol{z} = -(\mathcal{H} \otimes \boldsymbol{I})(\xi + \zeta + \boldsymbol{e}) \Rightarrow \xi + \zeta = -(\mathcal{H}^{-1} \otimes \boldsymbol{I})\boldsymbol{z} - \boldsymbol{e}$ in (19), and use the fact that $\frac{\boldsymbol{I}}{\delta_{\max}^2} \leq \mathcal{H}^{-2} \leq \frac{\boldsymbol{I}}{\delta_{\min}^2}$, one can obtain

$$\begin{aligned} & -\epsilon(\|\xi\|^2 + \|\zeta\|^2) \\ & \leq -\frac{\epsilon}{2}(\boldsymbol{z}^T(\mathcal{H}^{-2} \otimes \boldsymbol{I})\boldsymbol{z} + \boldsymbol{e}^T\boldsymbol{e}) - \epsilon \boldsymbol{z}^T(\mathcal{H}^{-1} \otimes \boldsymbol{I})\boldsymbol{e} \\ & \leq -\frac{\epsilon}{2\delta_{\max}^2}\boldsymbol{z}^T\boldsymbol{z} - \frac{\epsilon}{2}\boldsymbol{e}^T\boldsymbol{e} - \epsilon \boldsymbol{z}^T(\mathcal{H}^{-1} \otimes \boldsymbol{I})\boldsymbol{e} \end{aligned} \tag{20}$$

Using the relation that $-\epsilon \boldsymbol{z}^T(\mathcal{H}^{-1} \otimes \boldsymbol{I})\boldsymbol{e} \leq \epsilon(k\boldsymbol{e}^T(\mathcal{H}^{-2} \otimes \boldsymbol{I}_n)\boldsymbol{e} + \frac{1}{k}\boldsymbol{z}^T\boldsymbol{z}) \leq \epsilon\left(k\frac{1}{\delta_{min}^2}\boldsymbol{e}^T\boldsymbol{e} + \frac{1}{k}\boldsymbol{z}^T\boldsymbol{z}\right)$, (20) becomes

$$\begin{aligned} & -\epsilon(\|\xi\|^2 + \|\zeta\|^2) \\ & \leq \left(\frac{\epsilon}{k} - \frac{\epsilon}{2\delta_{\max}^2}\right)\boldsymbol{z}^T\boldsymbol{z} + \left(\frac{\epsilon k}{\delta_{min}^2} - \frac{\epsilon}{2}\right)\boldsymbol{e}^T\boldsymbol{e}, k > 0 \end{aligned} \tag{21}$$

which implies that

$$\boldsymbol{\delta}^T\boldsymbol{S}\boldsymbol{\delta} \leq \left(\frac{\epsilon}{k} - \frac{\epsilon}{2\delta_{\max}^2}\right)\boldsymbol{z}^T\boldsymbol{z} + \left(\frac{\epsilon k}{\delta_{\min}^2} - \frac{\epsilon}{2}\right)\boldsymbol{e}^T\boldsymbol{e} \tag{22}$$

Substituting (22) into (17), one can obtain

$$\begin{aligned} \dot{V} \leq & \left(\frac{\epsilon}{k} - \frac{\epsilon}{2\delta_{\max}^2}\right)\boldsymbol{z}^T\boldsymbol{z} + \left(\frac{\epsilon k}{\delta_{\min}^2} - \frac{\epsilon}{2}\right)\boldsymbol{e}^T\boldsymbol{e} \\ & + \boldsymbol{e}^T\left(\frac{\mathcal{H}^2}{b_1} \otimes \boldsymbol{M}_1^T\boldsymbol{M}_1 + \frac{\boldsymbol{\Theta}^2}{b_2} \otimes \boldsymbol{M}_2^T\boldsymbol{M}_2\right)\boldsymbol{e} \\ & - 2\boldsymbol{e}^T(\boldsymbol{\Theta} \otimes \boldsymbol{M}_3 - \boldsymbol{I}_N \otimes \boldsymbol{M}_1)\boldsymbol{z} \\ & + 2\boldsymbol{e}^T(\boldsymbol{\Theta} \otimes \boldsymbol{P}_3\boldsymbol{A} + \mathcal{H} \otimes \boldsymbol{M}_1)\boldsymbol{e} + \boldsymbol{e}^T(\dot{\boldsymbol{\Theta}} \otimes \boldsymbol{P}_3)\boldsymbol{e} \end{aligned} \tag{23}$$

Now the expression (23) consists only of accessible information $\boldsymbol{e}$ (measurement errors) and $\boldsymbol{z}$ (control inputs). To obtain a distributed rule, the last step is to diagonalize (23) by using the following two inequalities: $\mathcal{H}^2 \leq \delta_{\max}^2\boldsymbol{I}$ and $\boldsymbol{e}^T(\mathcal{H} \otimes \boldsymbol{M}_1)\boldsymbol{e} \leq \delta_{\max}\|\boldsymbol{M}_1\|\boldsymbol{e}^T\boldsymbol{e}$. Thus, (23) becomes

$$\dot{V} \leq \sum_{i=1}^{N}\left(\boldsymbol{e}_i^T\boldsymbol{Q}\boldsymbol{e}_i + \Pi_1\|\boldsymbol{z}_i\|^2 + \boldsymbol{e}_i^T\boldsymbol{\Pi}_2\boldsymbol{z}_i + \Pi_3\dot{\theta}_i\right) \tag{24}$$

where $\Pi_1 = \frac{\epsilon}{k} - \frac{\epsilon}{2\delta_{\max}^2}$, $\boldsymbol{\Pi}_2 = -2\theta_i\boldsymbol{M}_3 + 2\boldsymbol{M}_1$, $\Pi_3 = \boldsymbol{e}_i^T\boldsymbol{P}_3\boldsymbol{e}_i$, and $\boldsymbol{Q}$ is

$$\begin{aligned} \boldsymbol{Q} = & \left(\frac{\epsilon k}{\delta_{\min}^2} - \frac{\epsilon}{2} + 2\delta_{\max}\|\boldsymbol{M}_1\|\right)\boldsymbol{I}_n + 2\theta_i\boldsymbol{P}_3\boldsymbol{A} \\ & + \frac{\delta_{\max}^2}{b_1}\boldsymbol{M}_1^T\boldsymbol{M}_1 + \frac{\theta_i^2}{b_2}\boldsymbol{M}_2^T\boldsymbol{M}_2 \end{aligned} \tag{25}$$

Enforcing (24) being negative and one can obtain that $\dot{\theta}_i(t) < \omega_i(t)$ with $\omega_i(t)$ defined in (11). One can also verify the negativity of (24) by substituting (10) in (24) and then $\dot{V} \leq -\sum_i \tau_i < 0$. Therefore, the closed-loop system (7) is asymptotically stable, and the MAS (1) reaches leader-following consensus, which completes the proof. □

Remark 2. Notice that this strategy is distributed; thus, each agent determines its triggering moments according to its local information, facilitating algorithm implementation.

Remark 3. The main difficulty lies in the determination of $\boldsymbol{K}$ and $\boldsymbol{L}_o$, which involves a set of $\mathcal{BMIs}$ (8). These equations can be numerically challenging to solve. In Section 4.3, these $\mathcal{BMIs}$ are transferred to $\mathcal{LMIs}$, which facilitates the numerical computation.

The following Algorithm 1 shows the pseudo-code to implement the proposed theorem.

Algorithm 1 Implementation of distributed DETM control

Input:
  Communication topology: $\mathcal{H}$
  MAS model: $\boldsymbol{A}, \boldsymbol{B}, \boldsymbol{C}$
  $\boldsymbol{K}, \boldsymbol{L}_o, \boldsymbol{P}_1, \boldsymbol{P}_2, \boldsymbol{P}_3, \boldsymbol{S}$ and ϵ via Theorem 1
Initialize:
  for each follower agent i, $\tilde{\boldsymbol{x}}_i(0)$, $\hat{\boldsymbol{x}}_i(0)$, $\tilde{\boldsymbol{x}}_j(0), j \in \mathcal{N}_i$, $\hat{\boldsymbol{x}}_j(0)$, $\boldsymbol{e}_i(0) = \boldsymbol{0}$, $\theta_i(0) = \bar{\theta}_i$.
loop
  for every agent i **do**
    Get output $\boldsymbol{y}_i$
    Update $\tilde{\boldsymbol{x}}_i$ (according to (3)), $\hat{\boldsymbol{x}}_i$ (according to (5)) and $\boldsymbol{e}_i = \hat{\boldsymbol{x}}_i - \tilde{\boldsymbol{x}}_i$.
    Check event-triggered condition:
    if $\theta_i \leq 0$ **then**
      $\theta_i \leftarrow \bar{\theta}_i$, $\hat{\boldsymbol{x}}_i \leftarrow \tilde{\boldsymbol{x}}_i$, $\boldsymbol{e}_i \leftarrow \boldsymbol{0}$
      Broadcast $\tilde{\boldsymbol{x}}_i$ to its neighbors
    else
      Update θ_i according to (10)
    end if
    if Receive message from the neighbor j **then**
      Update $\hat{\boldsymbol{x}}_j \leftarrow \tilde{\boldsymbol{x}}_j$
    end if
    Update $\boldsymbol{z}_i$, $\boldsymbol{u}_i$ according to (4)
    (state update for agent i)
  end for
end loop

19346093, 0, Downloaded from https://onlinelibrary.wiley.com/doi/10.1002/asjc.3385 by Universite Paris-Saclay, Wiley Online Library on [29/04/2024]. See the Terms and Conditions (https://onlinelibrary.wiley.com/terms-and-conditions) on Wiley Online Library for rules of use; OA articles are governed by the applicable Creative Commons License

19346093, 0, Downloaded from https://onlinelibrary.wiley.com/doi/10.1002/asjc.3385 by Universite Paris-Saclay, Wiley Online Library on [29/04/2024]. See the Terms and Conditions (https://onlinelibrary.wiley.com/terms-and-conditions) on Wiley Online Library for rules of use; OA articles are governed by the applicable Creative Commons License

4.2 | Minimum interevent time control

In the following corollary, an explicit expression of MIET is deduced, and it is proved that the Zeno behavior does not exist under Theorem (1).

Corollary 1. *Under Theorem 1, the interevent time of agent i is lower-bounded by* $t^i_{\min}$ *defined as*

$$t^i_{\min} = \int_0^{\bar{\theta}_i} \frac{\mathrm{d}h}{\max(c_0 + c_1 h + c_2 h^2, 0) + \tau_i} \tag{26}$$

where $c_0 = \frac{1}{\eta}\left(\frac{\epsilon k}{\delta^2_{\min}} - \frac{\epsilon}{2} + \frac{\phi_1}{b_1} + 2\delta_{\max}\rho_1 + \frac{\rho_1^2}{\sigma_1}\right)$, $c_1 = \frac{\alpha}{\eta}$, $c_2 = \frac{1}{\eta}\left(\frac{\phi_2}{b_2} + \frac{\rho_3^2}{\sigma_2}\right)$, $\alpha = \lambda_{\max}(\boldsymbol{P}_3\boldsymbol{A} + \boldsymbol{A}^T\boldsymbol{P}_3)$, $\eta = \lambda_{\min}(\boldsymbol{P}_3)$, $\phi_1 = \lambda_{\max}(\mathcal{H}^2 \otimes \boldsymbol{M}_1^T\boldsymbol{M}_1)$, $\phi_2 = \lambda_{\max}(\boldsymbol{M}_2^T\boldsymbol{M}_2)$, $\rho_1 = \|\boldsymbol{M}_1\|$, $\rho_3 = \|\boldsymbol{M}_3\|$, $k > 2\delta^2_{\max}$, *and* σ_1, σ_2 *are two positive scalars satisfying*

$$\frac{\epsilon}{2\delta^2_{\max}} - \frac{\epsilon}{k} - \sigma_1 - \sigma_2 = 0 \tag{27}$$

Proof. By (11), a lower bound of ω_i could be found by using the following expressions:

$$\boldsymbol{e}_i^T\boldsymbol{P}_3\boldsymbol{e}_i \geq \eta\|\boldsymbol{e}_i\|^2 \tag{28}$$

$$\begin{aligned} &\boldsymbol{e}_i^T\boldsymbol{Q}\boldsymbol{e}_i \\ &\leq \boldsymbol{e}_i^T\boldsymbol{e}_i\left(\frac{\epsilon k}{\delta^2_{\min}} - \frac{\epsilon}{2} + 2\delta_{\max}\rho_1 + \alpha\theta_i + \frac{\phi_1}{b_1} + \frac{\phi_2}{b_2}\theta_i^2\right) \end{aligned} \tag{29}$$

and

$$\begin{aligned} &-\boldsymbol{e}_i^T(2\boldsymbol{M}_1 - 2\theta_i\boldsymbol{M}_3)\boldsymbol{z}_i = -2\boldsymbol{e}_i^T\boldsymbol{M}_1\boldsymbol{z}_i + 2\boldsymbol{e}_i^T\theta_i\boldsymbol{M}_3\boldsymbol{z}_i \\ &\geq -\frac{1}{\sigma_1}\rho_1^2\|\boldsymbol{e}_i\|^2 - \sigma_1\|\boldsymbol{z}_i\|^2 - \frac{1}{\sigma_2}\theta_i^2\rho_3^2\|\boldsymbol{e}_i\|^2 - \sigma_2\|\boldsymbol{z}_i\|^2 \\ &= -\left(\frac{1}{\sigma_2}\theta_i^2\rho_3^2 + \frac{1}{\sigma_1}\rho_1^2\right)\|\boldsymbol{e}_i\|^2 - (\sigma_1 + \sigma_2)\|\boldsymbol{z}_i\|^2 \end{aligned} \tag{30}$$

Substituting (28)–(30) into (11) and using the relation that $\frac{\epsilon}{2\delta^2_{\max}} - \frac{\epsilon}{k} - \sigma_1 - \sigma_2 = 0$, one can obtain $\omega_i \geq -\frac{1}{\eta}\left(\frac{\epsilon k}{\delta^2_{\min}} - \frac{\epsilon}{2} + \frac{\phi_1}{b_1} + 2\delta_{\max}\rho_1 + \frac{\rho_1^2}{\sigma_1}\right) - \frac{\alpha}{\eta}\theta_i - \left(\frac{1}{\eta}\left(\frac{\phi_2}{b_2} + \frac{\rho_3^2}{\sigma_2}\right)\right)\theta_i^2 = -\left(c_0 + c_1\theta_i + c_2\theta_i^2\right)$, then one can conclude that the time required for θ_i descending from $\bar{\theta}_i$ to 0 is lower bounded by

$$t^i_{\min} = \int_{\bar{\theta}_i}^{0} \frac{\mathrm{d}h}{\min(-(c_0 + c_1 h + c_2 h^2), 0) - \tau_i} \tag{31}$$

which is equivalent to (26). □

Remark 4. The numerical value of $t^i_{\min}$ can be determined through numerical integration or analytical integration provided that $c_0 + c_1 h + c_2 h^2 \geq 0, h \in [0, \bar{\theta}_i]$. In the latter method, the analytical integration depends on the discriminant of $(c_0 + \tau_i) + c_1 h + c_2 h^2 = 0$, where its roots (could be complex numbers) are denoted as h_1 and h_2. Notice that c_0, c_1, c_2 are all positive and $(c_0 + \tau_i) + c_1 h + c_2 h^2 > 0$. In this case, $t^i_{\min}$ can be expressed in (32).

$$t^i_{\min} = \begin{cases} \frac{1}{c_2(h_1 - h_2)}\ln\left(\frac{h_2(\bar{\theta}_i - h_1)}{h_1(\bar{\theta}_i - h_2)}\right), & \text{if } \Delta > 0 \\ -\frac{1}{c_2}\left(\frac{1}{h_1} + \frac{1}{\bar{\theta}_i - h_1}\right), & \text{if } \Delta = 0 \\ \frac{2}{\sqrt{-\Delta}}\left[\mathrm{at}\left(\frac{2c_2\bar{\theta}_i + c_1}{\sqrt{-\Delta}}\right) - \mathrm{at}\left(\frac{c_1}{\sqrt{-\Delta}}\right)\right], \\ \text{if } \Delta < 0 \end{cases} \tag{32}$$

where $\Delta = c_1^2 - 4(c_0 + \tau_i)c_2$, at(•) denotes the function arctan(•).

Corollary 1 implies that the Zeno behavior of the proposed DETM is excluded. Notice that there is also a limitation of $t^i_{\min}$ when $\bar{\theta}_i$ approaches to positive infinity. By adjusting the value of $\bar{\theta}_i$, one can vary the MIET and maintain the event frequency consistently lower than $1/t^i_{\min}$. Increasing the value of $\bar{\theta}_i$ enables the interevent time as long as possible not to overload the communication network. Indeed, a smaller $\bar{\theta}_i$ could also be designed to keep better surveillance and a higher convergence speed if the network allows it. Therefore, by choosing an appropriate parameter $\bar{\theta}_i$, the control performance and the communication frequency could achieve a good compromise.

Indeed, under the event-triggered strategy, the control performance (regarding the convergence speed) is no better than continuous control. This degradation cannot be avoided. The advantage of the proposed method is that for systems that do not require high convergence speed, one can adjust the parameter $\bar{\theta}_i$ to minimize communication frequency. On the contrary, for systems that demand high convergence speed, the event frequency cannot be set too low. Indeed, this method has the advantage of

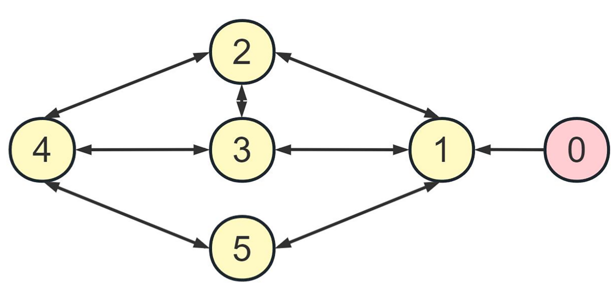

FIGURE 1 Communication topology. [Color figure can be viewed at wileyonlinelibrary.com]

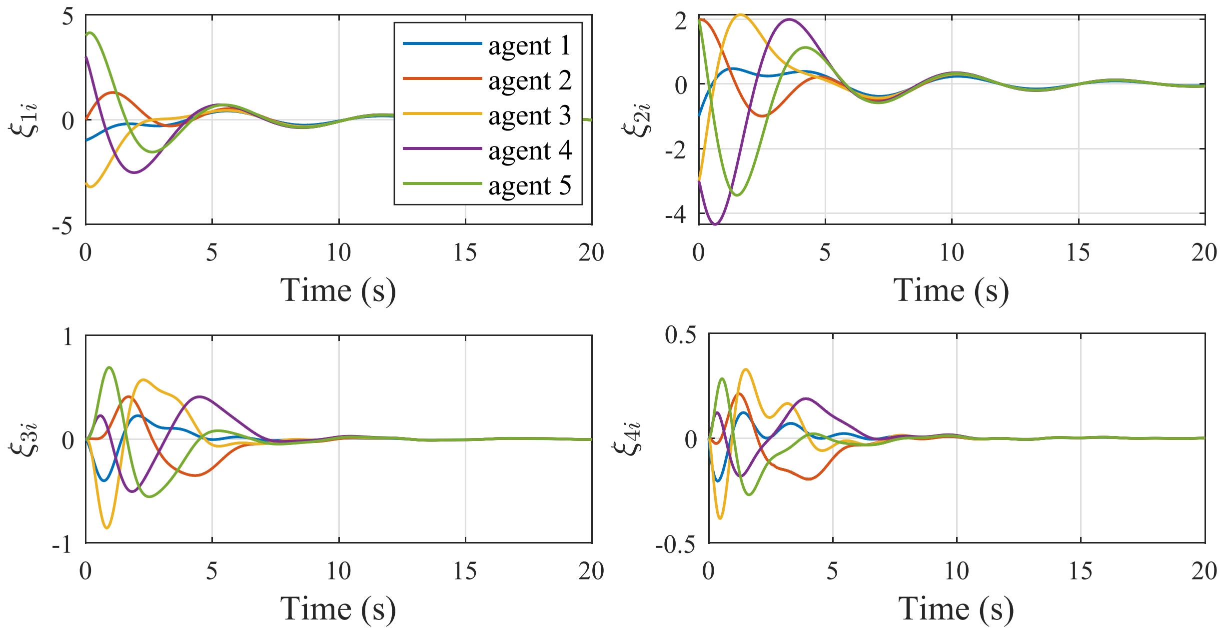

FIGURE 2 Consensus error of follower agents. [Color figure can be viewed at wileyonlinelibrary.com]

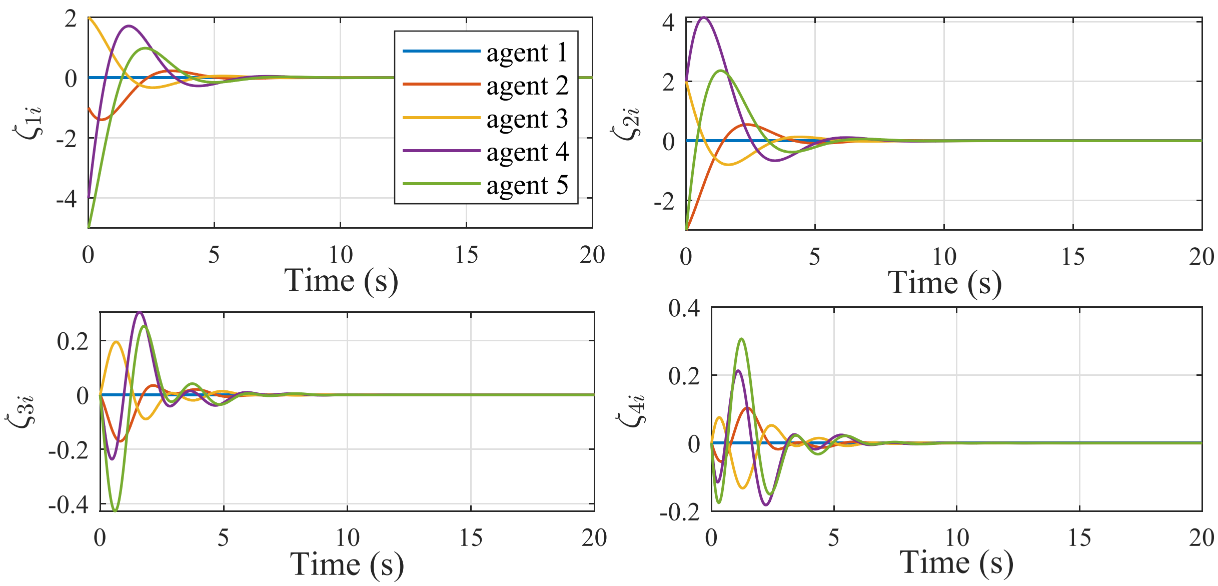

FIGURE 3 Observer state error of follower agents. [Color figure can be viewed at wileyonlinelibrary.com]

conveniently adjusting the balance between control performance and resource scheduling according to practical needs.

4.3 | Linear matrix inequality (LMI)-based sufficient conditions

Solving the $\mathcal{BMI}$s in Theorem 1 could be challenging and may need a lot of attempts through numerical iterations. This section proposes sufficient conditions of $\mathcal{LMI}$s to solve $\mathcal{BMI}$s in Theorem 1, which simplifies the numerical computation.

Corollary 2. *The $\mathcal{BMI}$s in Theorem 1 are satisfied if the $\mathcal{LMI}$s in (33) are satisfied with regard to $\boldsymbol{P}_1 > 0$, $\boldsymbol{P}_2 > 0$, $\boldsymbol{K}$ and $\boldsymbol{F}$, where b_1, b_2, μ_1 are arbitrary positive scalars. Then the observer gain is obtained as $\boldsymbol{L}_o = \boldsymbol{P}_2^{-1}\boldsymbol{F}$.*

$$\begin{cases} \boldsymbol{\Omega} = \begin{pmatrix} \boldsymbol{\Omega}_{11} & \boldsymbol{0}_{Nn} & \mathcal{H}\otimes(\boldsymbol{P}_1\boldsymbol{B}) & \boldsymbol{\Omega}_{14} \\ * & \boldsymbol{\Omega}_{22} & -\boldsymbol{I}_N\otimes\boldsymbol{K}^T & \boldsymbol{0}_{Nn} \\ * & * & -2\boldsymbol{I}_{Nm} & \boldsymbol{0}_{Nm\times Nn} \\ * & * & * & -\boldsymbol{I}_{Nn} \end{pmatrix} < 0 \\ \boldsymbol{\Omega}_{11} = \boldsymbol{I}_N\otimes(\boldsymbol{P}_1\boldsymbol{A}+\boldsymbol{A}^T\boldsymbol{P}_1)+\boldsymbol{I}_{Nn}-2\frac{\boldsymbol{I}_N\otimes\boldsymbol{P}_1}{\mu_1} \\ \boldsymbol{\Omega}_{14} = \frac{\boldsymbol{I}_N\otimes\boldsymbol{P}_1}{\mu_1}-\mu_1\mathcal{H}\otimes(\boldsymbol{K}^T\boldsymbol{B}^T) \\ \boldsymbol{\Omega}_{22} = \boldsymbol{I}_N\otimes(\boldsymbol{P}_2\boldsymbol{A}+\boldsymbol{A}^T\boldsymbol{P}_2+\boldsymbol{F}\boldsymbol{C}+\boldsymbol{C}^T\boldsymbol{F}^T)+(b_1+b_2)\boldsymbol{I}_{Nn} \end{cases} \tag{33}$$

19346093, 0, Downloaded from https://onlinelibrary.wiley.com/doi/10.1002/asjc.3385 by Universite Paris-Saclay, Wiley Online Library on [29/04/2024]. See the Terms and Conditions (https://onlinelibrary.wiley.com/terms-and-conditions) on Wiley Online Library for rules of use; OA articles are governed by the applicable Creative Commons License

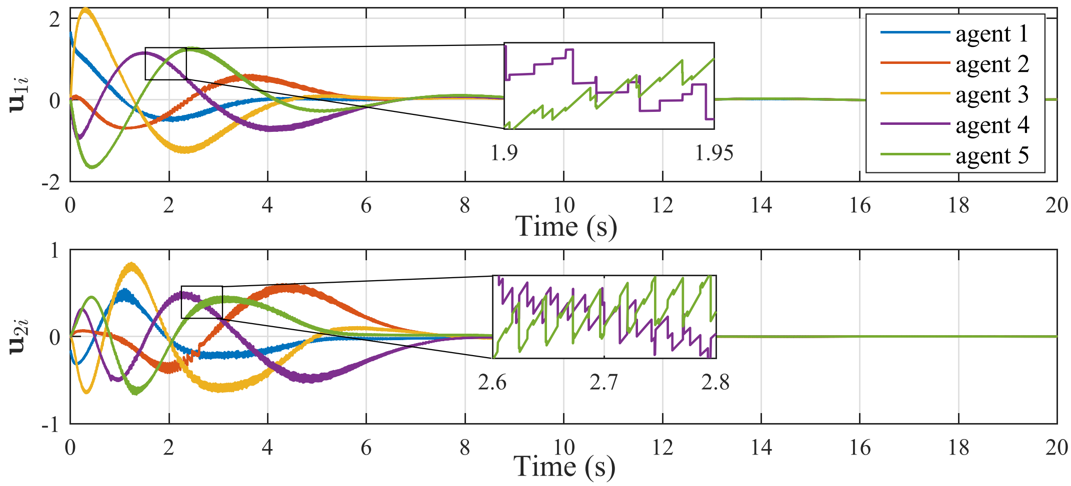

FIGURE 4 Control input of follower agents. [Color figure can be viewed at wileyonlinelibrary.com]

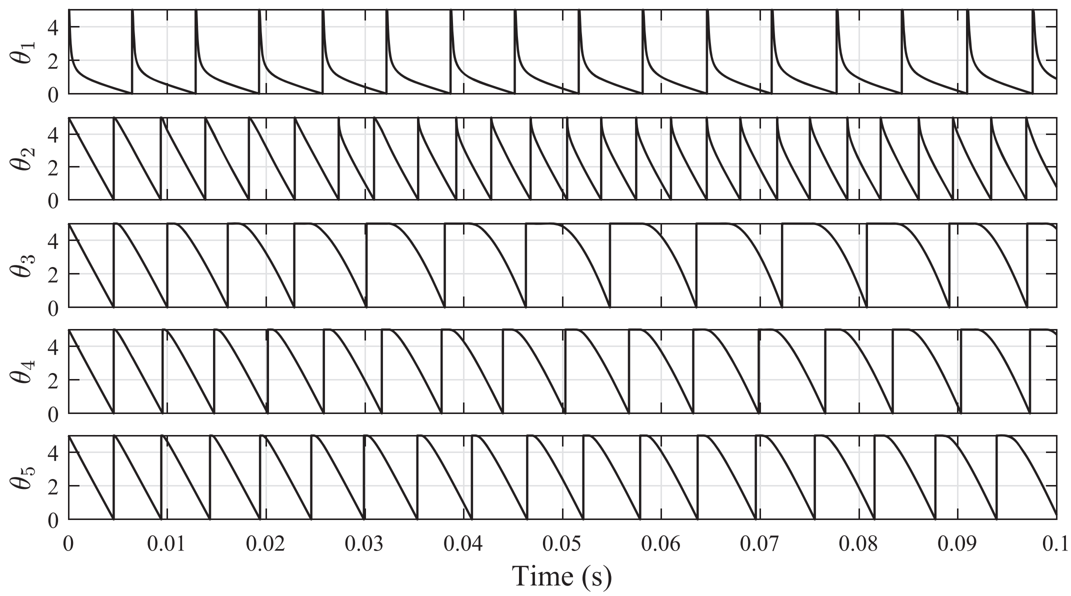

FIGURE 5 Time evolution of ADV $\theta_i(t)$ of follower agents. ADV, auxiliary dynamic variable.

Proof. One can first make a change of variable of $\boldsymbol{F} = \boldsymbol{P}_2\boldsymbol{L}_o$ in (8); thus, the term $\boldsymbol{S}_{22}$ in $\boldsymbol{S}$ (8) becomes $\boldsymbol{\Omega}_{22}$. Notice that the matrix $\boldsymbol{S}$ in Theorem 1 could be decomposed into $\boldsymbol{S} = \boldsymbol{\Gamma}^T\boldsymbol{\Lambda}\boldsymbol{\Gamma}$ with $\boldsymbol{\Gamma}$ and $\boldsymbol{\Lambda}$ defined as

$$\boldsymbol{\Gamma} = \begin{pmatrix} \boldsymbol{I}_{Nn} & \boldsymbol{0}_{Nn} \\ \boldsymbol{0}_{Nn} & \boldsymbol{I}_{Nn} \\ \boldsymbol{0}_{Nm\times Nn} & -\boldsymbol{I}_N \otimes \boldsymbol{K} \end{pmatrix}, \boldsymbol{\Lambda} = \begin{pmatrix} \boldsymbol{\Lambda}_{11} & \boldsymbol{0}_{Nn} & \mathcal{H} \otimes \boldsymbol{P}_1\boldsymbol{B} \\ * & \boldsymbol{\Omega}_{22} & -\boldsymbol{I}_N \otimes \boldsymbol{K}^T \\ * & * & -2\boldsymbol{I}_{Nn} \end{pmatrix} \tag{34}$$

where $\boldsymbol{\Lambda}_{11} = \boldsymbol{I}_N \otimes (\boldsymbol{P}_1\boldsymbol{A} + \boldsymbol{A}^T\boldsymbol{P}_1) - \mathcal{H} \otimes (\boldsymbol{P}_1\boldsymbol{BK} + \boldsymbol{K}^T\boldsymbol{B}^T\boldsymbol{P}_1)$. Thus, $\boldsymbol{\Lambda} < 0$ is a sufficient condition for $\boldsymbol{S} < 0$. To find a $\mathcal{LMI}$ form, the idea is to separate $\boldsymbol{P}_1$ and $\boldsymbol{K}$ in the left-top block of $\boldsymbol{\Lambda}$. The following inequalities are established:

$$\begin{aligned} & -\mathcal{H} \otimes (\boldsymbol{P}_1\boldsymbol{BK} + \boldsymbol{K}^T\boldsymbol{B}^T\boldsymbol{P}_1) \\ \leq & -\mathcal{H} \otimes (\boldsymbol{P}_1\boldsymbol{BK} + \boldsymbol{K}^T\boldsymbol{B}^T\boldsymbol{P}_1) + (\mu_1^2\mathcal{H}^2) \otimes (\boldsymbol{K}^T\boldsymbol{B}^T\boldsymbol{BK}) \\ \leq & \left(\frac{\boldsymbol{I}_N \otimes \boldsymbol{P}_1}{\mu_1} - \mu_1\mathcal{H} \otimes \boldsymbol{BK}\right)^T \left(\frac{\boldsymbol{I}_N \otimes \boldsymbol{P}_1}{\mu_1} - \mu_1\mathcal{H} \otimes \boldsymbol{BK}\right) \\ & -\frac{\boldsymbol{I}_N \otimes \boldsymbol{P}_1^2}{\mu_1^2}, \quad \mu_1 > 0 \end{aligned} \tag{35}$$

and

$$-(\boldsymbol{I}_N \otimes \boldsymbol{P}_1^2)/\mu_1^2 \leq \boldsymbol{I}_{Nn} - 2(\boldsymbol{I}_N \otimes \boldsymbol{P}_1)/\mu_1 \tag{36}$$

then one can have

19346093, 0, Downloaded from https://onlinelibrary.wiley.com/doi/10.1002/asjc.3385 by Universite Paris-Saclay, Wiley Online Library on [29/04/2024]. See the Terms and Conditions (https://onlinelibrary.wiley.com/terms-and-conditions) on Wiley Online Library for rules of use; OA articles are governed by the applicable Creative Commons License

19346093, 0, Downloaded from https://onlinelibrary.wiley.com/doi/10.1002/asjc.3385 by Universite Paris-Saclay, Wiley Online Library on [29/04/2024]. See the Terms and Conditions (https://onlinelibrary.wiley.com/terms-and-conditions) on Wiley Online Library for rules of use; OA articles are governed by the applicable Creative Commons License

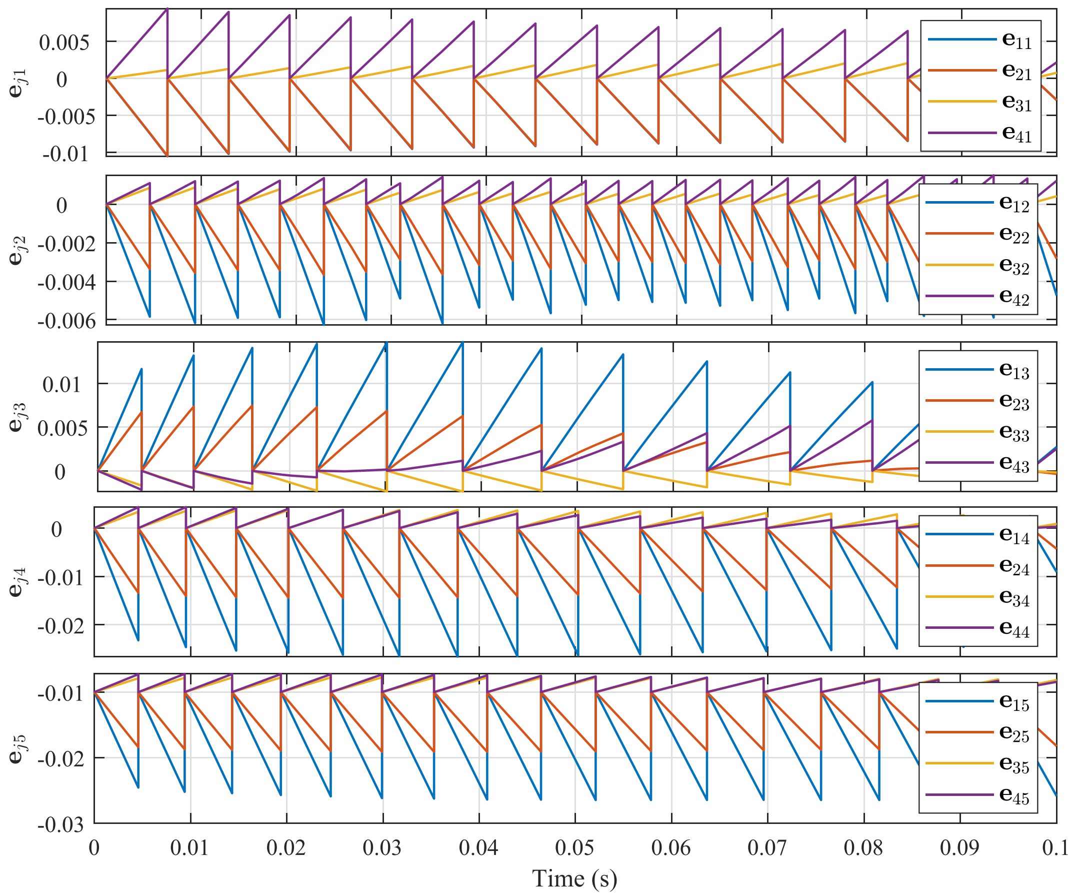

FIGURE 6 Measurement error of follower agents. [Color figure can be viewed at wileyonlinelibrary.com]

TABLE 1 Interevent time (in ms) using different $\bar{\theta}_i$ under the proposed DETM and SETM: mean values (mean), minimum values (Min), and maximum values (Max) among five follower agents.

	DETM different $\bar{\theta}_i$ values					
Case	**0.1**	**1**	**5**	**100**	**500**	**SETM**
Mean	0.14	8.79	13.27	16.22	16.35	1.11
Min	0.069	6.66	12.63	13.14	13.14	0.61
Max	5.56	12.44	14.31	20.73	21.14	3.57

Abbreviations: DETM, dynamic event-triggered mechanism; SETM, static event-triggered mechanism.

$$
\begin{aligned}
&\boldsymbol{I}_N \otimes (\boldsymbol{P}_1\boldsymbol{A} + \boldsymbol{A}^T\boldsymbol{P}_1) - \mathcal{H} \otimes (\boldsymbol{P}_1\boldsymbol{B}\boldsymbol{K} + \boldsymbol{K}^T\boldsymbol{B}^T\boldsymbol{P}_1) \\
&\leq \boldsymbol{I}_N \otimes (\boldsymbol{P}_1\boldsymbol{A} + \boldsymbol{A}^T\boldsymbol{P}_1) + \left(\frac{\boldsymbol{I}_N \otimes \boldsymbol{P}_1}{\mu_1} - \mu_1\mathcal{H} \otimes \boldsymbol{B}\boldsymbol{K}\right)^T \\
&\times \left(\frac{\boldsymbol{I}_N \otimes \boldsymbol{P}_1}{\mu_1} - \mu_1\mathcal{H} \otimes \boldsymbol{B}\boldsymbol{K}\right) + \boldsymbol{I}_{Nn} - 2\frac{\boldsymbol{I}_N \otimes \boldsymbol{P}_1}{\mu_1}
\end{aligned} \tag{37}
$$

Thus, by using (37) in $\boldsymbol{\Lambda}$ (34) and the Schur complement, one can obtain the matrix $\boldsymbol{\Omega}$ in (33). □

Remark 5. The introduction of the inequality constraint (36), and then the presence of the positive term $\boldsymbol{I}_{Nn}$ in $\boldsymbol{\Omega}_{11}$, makes the result of Corollary 2 conservative. In the following corollary, a new representation of $\mathcal{LMI}s$ with less conservatism is proposed.

Corollary 3. *The $\mathcal{BMI}s$ in Theorem 1 are satisfied if the following conditions are satisfied:*

1. *$\boldsymbol{B}$ has full column rank.*
2. *The following $\mathcal{LMI}s$ are satisfied with regard to $\boldsymbol{P}_1 > 0$, $\boldsymbol{P}_2 > 0$, $\boldsymbol{N}$, $\boldsymbol{R}$ and $\boldsymbol{F}$:*

$$
\begin{cases}
\boldsymbol{\Xi} = \begin{pmatrix} \boldsymbol{\Xi}_{11} & \boldsymbol{\Xi}_{12} \\ * & \boldsymbol{\Xi}_{22} \end{pmatrix} < 0 \\
\boldsymbol{\Xi}_{11} = \boldsymbol{I}_N \otimes (\boldsymbol{P}_1\boldsymbol{A} + \boldsymbol{A}^T\boldsymbol{P}_1) - \mathcal{H} \otimes (\boldsymbol{B}\boldsymbol{N} + \boldsymbol{N}^T\boldsymbol{B}^T) \\
\boldsymbol{\Xi}_{12} = -\mathcal{H} \otimes \boldsymbol{B}\boldsymbol{N} \\
\boldsymbol{\Xi}_{22} = \boldsymbol{I}_N \otimes (\boldsymbol{P}_2\boldsymbol{A} + \boldsymbol{A}^T\boldsymbol{P}_2 + \boldsymbol{F}\boldsymbol{C} + \boldsymbol{C}^T\boldsymbol{F}^T) + (b_1 + b_2)\boldsymbol{I}_{Nn} \\
\boldsymbol{B}\boldsymbol{R} = \boldsymbol{P}_1\boldsymbol{B}
\end{cases} \tag{38}
$$

where b_1, b_2 are two arbitrary positive scalar. Then $\boldsymbol{K}, \boldsymbol{L}_o$ are obtained as $\boldsymbol{K} = \boldsymbol{R}^{-1}\boldsymbol{N}$, $\boldsymbol{L}_o = \boldsymbol{P}_2^{-1}\boldsymbol{F}$.

Proof. One can first perform a change of variable of $\boldsymbol{F} = \boldsymbol{P}_2\boldsymbol{L}_o$ in (8); thus, the term $\boldsymbol{S}_{22}$ in $\boldsymbol{S}$ (8) becomes $\boldsymbol{\Xi}_{22}$. Since $\boldsymbol{B}$ is assumed with full column rank, then it

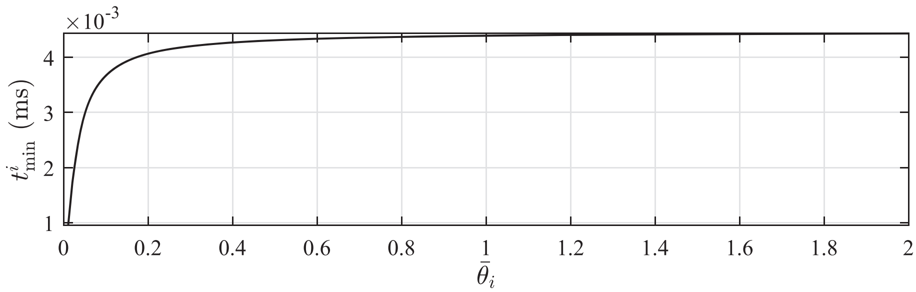

FIGURE 7 Minimum interevent time $t^i_{\min}$ with different $\bar{\theta}_i$ using (26).

follows from the linear matrix equality ($\mathcal{LME}$) $\boldsymbol{BR} = \boldsymbol{P}_1\boldsymbol{B}$ that $\boldsymbol{R}$ is a regular matrix [39]. Using the change of variable $\boldsymbol{N} = \boldsymbol{RK}$, one can have

$$\begin{aligned} &I_N \otimes (\boldsymbol{P}_1\boldsymbol{A} + \boldsymbol{A}^T\boldsymbol{P}_1) - \mathcal{H} \otimes (\boldsymbol{P}_1\boldsymbol{BK} + \boldsymbol{K}^T\boldsymbol{B}^T\boldsymbol{P}_1) \\ &= I_N \otimes (\boldsymbol{P}_1\boldsymbol{A} + \boldsymbol{A}^T\boldsymbol{P}_1) - \mathcal{H} \otimes (\boldsymbol{BN} + \boldsymbol{N}^T\boldsymbol{B}^T) \end{aligned} \tag{39}$$

thus, one can get Ξ, which completes the proof. □

Remark 6. It is worth noting that Corollary 3 is derived based on the equality constraint $BR = P_1B$ and by removing the inequality (36). Indeed, the proposed result is more relaxed compared with the Corollary 2.

Remark 7. In Corollary 3, it is assumed that $\boldsymbol{B}$ has full column rank. This property exists in many autonomous systems such as quadrotor UAVs, VTOL aircraft, and autonomous ground vehicles. Nevertheless, the matrix $\boldsymbol{B}$ should always be carefully examined, especially when dealing with overactuated systems such as octorotor UAVs.

5 | NUMERICAL EXAMPLES AND DISCUSSIONS

This section demonstrates simulations using the same homogeneous MAS as in Trejo et al. [6] with the following matrices:

$$\boldsymbol{A} = \begin{pmatrix} -0.05 & 1 & 0 & 0 \\ -1 & 0 & 0 & 0 \\ 0 & 0 & 0 & 3 \\ 0 & 0 & -3 & 0 \end{pmatrix}, \boldsymbol{B} = \begin{pmatrix} 1 & 0 \\ 1 & 0 \\ 0 & 1 \\ -1 & -1 \end{pmatrix}, \boldsymbol{C} = \begin{pmatrix} 1 & 0 \\ 0 & 0 \\ 0 & 1 \\ 0 & 0 \end{pmatrix}^T \tag{40}$$

The agents' initial conditions are set as $\boldsymbol{x}_0(0) = [1100]^T, \boldsymbol{x}_1(0) = [0000]^T, \boldsymbol{x}_2(0) = [1300]^T, \boldsymbol{x}_3(0) = [-2-200]^T, \boldsymbol{x}_4(0) = [4-200]^T, \boldsymbol{x}_5(0) = [5300]^T$. The initial state of observers is set to 0.

Notation: The figures in this section use ϕ_{ji} to denote the jth dimension of agent i's vector $\boldsymbol{\phi}$.

The communication topology is illustrated in Figure 1. Notice that the leader agent is the root of the associated augmented graph $\bar{\mathcal{G}}$. The matrix $\mathcal{H} = \mathcal{L} + \mathcal{D}$ is calculated in (41).

$$\mathcal{H} = \begin{pmatrix} 4 & -1 & -1 & 0 & -1 \\ -1 & 3 & -1 & -1 & 0 \\ -1 & -1 & 3 & -1 & 0 \\ 0 & -1 & -1 & 3 & -1 \\ -1 & 0 & 0 & -1 & 2 \end{pmatrix} \tag{41}$$

Since the matrix $\boldsymbol{B}$ has full column rank, Theorem 1, Corollary 2, and Corollary 3 are all available to calculate matrices $\boldsymbol{K}$ and $\boldsymbol{L}_o$. Here Corollary 3 is applied with $b_1 = b_2 = 1$ and obtain the following solution:

$$\boldsymbol{P}_1 = \begin{pmatrix} 0.9637 & -0.0332 & -0.0687 & 0.0395 \\ -0.0332 & 0.7507 & -0.0661 & -0.0119 \\ -0.0687 & -0.0661 & 0.7261 & 0.0152 \\ 0.0395 & -0.0119 & 0.0152 & 0.7734 \end{pmatrix} \tag{42}$$

$$\boldsymbol{P}_2 = \begin{pmatrix} 9.4028 & -4.2287 & -0.1542 & 0.0768 \\ -4.2287 & 9.1795 & 0.2980 & -0.0497 \\ -0.1542 & 0.2980 & 7.4782 & -1.6851 \\ 0.0768 & -0.0497 & -1.6851 & 7.3205 \end{pmatrix} \tag{43}$$

$$\boldsymbol{K} = \begin{pmatrix} 0.8911 & -0.1082 \\ 0.7295 & -0.0542 \\ -0.1501 & 0.7108 \\ -0.7458 & -0.7581 \end{pmatrix}^T, \boldsymbol{L}_o = \begin{pmatrix} -1.2495 & 0.0145 \\ -0.7618 & 0.0766 \\ 0.1780 & -1.3524 \\ 0.2530 & -0.2746 \end{pmatrix} \tag{44}$$

Regarding the consensus error in Figure 2, it can be seen that the system achieves the consensus among the agents. The consensus error asymptotically diminishes over time. This outcome validates the effectiveness of our control strategy in driving the system toward a desired consensus. Simultaneously, the observer state error in Figure 3 demonstrates the convergence of the observer's estimated states to the actual states of the system. The diminishing observer state error signifies the accuracy and reliability of our observer design, which successfully tracks the true states of the system despite limited information availability. This highlights the practical significance of incorporating an observer in the control scheme, particularly in scenarios where direct state measurements are unattainable. Figure 4 represents the control inputs corresponding to the proposed event-triggered control strategy.

The time evolution of $\theta_i(t)$ is presented in Figure 5. It is evident that θ_i for each agent exhibits an asynchronous pattern. This phenomenon arises due to the distributed

19346093, 0, Downloaded from https://onlinelibrary.wiley.com/doi/10.1002/asjc.3385 by Universite Paris-Saclay, Wiley Online Library on [29/04/2024]. See the Terms and Conditions (https://onlinelibrary.wiley.com/terms-and-conditions) on Wiley Online Library for rules of use; OA articles are governed by the applicable Creative Commons License

nature of the MAS, where each agent operates independently based on its local information and interactions with neighboring agents. The events occur at the discontinuous points where θ_i is reset to $\bar{\theta}_i$, which shows a clock-like behavior. Figure 6 shows the evolution of the measurement error of each agent, where the discontinuous points imply events corresponding to those in Figure 5.

Table 1 concludes the interevent time using different event-triggered strategies: DETM from Theorem 1 and static event-triggered mechanism (SETM). For SETM, the Lyapunov function is the same as in the proof of Theorem 1 by taking $\boldsymbol{\Theta} = \boldsymbol{I}_N, \dot{\boldsymbol{\Theta}} = \boldsymbol{0}$, which finally leads to a static event-triggered rule. According to Table 1, the interevent time increases with larger $\bar{\theta}_i$ and can be easily tuned to be longer than SETM. For instance, the mean interevent time under $\bar{\theta}_i = 500$ is 16.345 ms (61 Hz), while for the static approach, it is 1.105 ms (904 Hz). Since the triggering frequency represents the usage of communication resources, in this scenario, one can save 93.23% of resource usage compared with the static strategy.

Figure 7 plots $t^i_{\min}$ with different $\bar{\theta}_i$ using (26). The proposed DETM prevents Zeno behavior as long as $\bar{\theta}_i > 0$. By adjusting $\bar{\theta}_i$, one can control the MIET and guarantee that the network communication is consistently below a designated frequency. Note that $t^i_{\min}$ is a lower bound on the interevent time. The actual average interevent time, as shown in Table 1, is significantly longer than the MIET. The MIET only serves as an indicator in the worst-case scenario.

6 | CONCLUSION

This paper presents an innovative approach to address the leader-following consensus problem for MASs using a dynamic event-triggered control protocol based on observers. Compared with the existing research, the proposed method incorporates distributed controllers, state observers, and event-triggered rules, which are synthesized using $\mathcal{LMI}$ terms. The developed techniques involve model-based estimation and clock-like ADVs to effectively prolong the interevent time, resulting in a significant performance improvement in interevent time. Additionally, an explicit expression for the minimum interevent time, enhancing more flexible tuning, is provided. Further research will focus on extending the proposed methods for MAS consensus problems subject to constraints. The effect of external disturbance and uncertainty will also be taken into consideration.

AUTHOR CONTRIBUTIONS

Zeyuan Wang: Investigation; methodology; software; validation; visualization; writing—original draft; writing—review and editing. **Mohammed Chadli:** Conceptualization; funding acquisition; supervision; validation; writing—original draft; writing—review and editing.

ACKNOWLEDGMENTS

The authors would like to express their sincere appreciation to the Associate Editor and the reviewers for their valuable suggestions and comments.

CONFLICT OF INTEREST STATEMENT

The authors declare no potential conflict of interests.

ORCID

Zeyuan Wang https://orcid.org/0000-0001-7211-9543
Mohammed Chadli https://orcid.org/0000-0002-0140-5187

REFERENCES

1. J. A. Vazquez Trejo, D. Rotondo, M. A. Medina, and D. Theilliol, *Observer-based event-triggered model reference control for multi-agent systems*, 2020 International Conference on Unmanned Aircraft Systems (ICUAS), IEEE, Athens, Greece, 2020, pp. 421–428 en.
2. W. Guo, M. Zou, and M. Li, *Distributed input observer-based consensus for the leader-following multi-agent systems*, Asian J. Control **22** (2020), no. 6, 2388–2394.
3. C. Wang, L. Zhang, and F. Cao, *Leader-following consensus control of second-order nonlinear multi-agent systems with applications to slew rate control*, Asian J. Control **25** (2023), no. 3, 2286–2294.
4. O. Cihan, *Stability analysis and controller design for consensus in discrete-time networks with heterogeneous agent dynamics*, Asian J. Control **25** (2023), 77–87.
5. V. T. J. Antonio, G. Adrien, A.-M. Manuel, P. Jean-Christophe, C. Laurent, R. Damiano, and T. Didier, *Event-triggered leader-following formation control for multi-agent systems under communication faults: application to a fleet of unmanned aerial vehicles*, J. Syst. Eng. Electron. **32** (2021), no. 5, 1014–1022.
6. J. A. V. Trejo, M. Chadli, D. Rotondo, M. A. Medina, and D. Theilliol, *Event-triggered fault-tolerant leader-following control for homogeneous multi-agent systems*, IFAC-PapersOnLine **55** (2022), no. 6, 79–84 en.
7. M. Zaeri Amirani, N. Bigdeli, and M. Haeri, *Distributed fault detection and isolation in time-varying formation tracking UAV multi-agent systems*, Asian J. Control **25** (2023), no. 1, 604–622.
8. K. Hanada, T. Wada, I. Masubuchi, T. Asai, and Y. Fujisaki, *Multi-agent consensus with stopping rules under bounded measurement noise*, Asian J. Control **25** (2023), no. 2, 651–661.
9. Y. Wang, J. Cao, and H. Wang, *Event-based impulsive consensus for delayed multi-agent systems*, Asian J. Control **24** (2022), no. 2, 771–781.
10. G. Wen, P. Wang, Y. Lv, G. Chen, and J. Zhou, *Secure consensus of multi-agent systems under denial-of-service attacks*, Asian J. Control **25** (2022), 695–709.
11. H. Gu, K. Liu, G. Zhu, and J. Lü, *Leader-following consensus of stochastic dynamical multi-agent systems with fixed and switching topologies under proportional-integral protocols*, Asian J. Control **25** (2022), 662–676.

1934693, 0, Downloaded from https://onlinelibrary.wiley.com/doi/10.1002/asjc.3385 by Universite Paris-Saclay, Wiley Online Library on [29/04/2024]. See the Terms and Conditions (https://onlinelibrary.wiley.com/terms-and-conditions) on Wiley Online Library for rules of use; OA articles are governed by the applicable Creative Commons License

12. A. Amirkhani and A. H. Barshooi, *Consensus in multi-agent systems: a review*, Artif. Intel. Rev. **55** (2021), 3897–3935.
13. A. Qiu, A. W. Al-Dabbagh, and T. Chen, *A tradeoff approach for optimal event-triggered fault detection*, IEEE Trans. Industr. Electron. **66** (2019), no. 3, 2111–2121.
14. P. Tabuada, *Event-triggered real-time scheduling of stabilizing control tasks*, IEEE Trans. Autom. Control **52** (2007), 1680–1685.
15. Y. Wu, X. Yang, H. Yan, M. Chadli, and Y. Wang, *Adaptive fuzzy event-triggered sliding mode control for uncertain euler-lagrange systems with performance specifications*, IEEE Trans. Fuzzy Syst. **31** (2022), 1566–1579.
16. D. V. Dimarogonas, E. Frazzoli, and K. H. Johansson, *Distributed event-triggered control for multi-agent systems*, IEEE Trans. Autom. Control **57** (2012), no. 5, 1291–1297.
17. X. Chen and F. Hao, *Event-triggered consensus control of second-order multi-agent systems*, Asian J. Control **17** (2015), no. 2, 592–603.
18. I. Ahmed, M. Rehan, N. Iqbal, and C. K. Ahn, *A novel event-triggered consensus approach for generic linear multi-agents under heterogeneous sector-restricted input nonlinearities*, IEEE Trans. Netw. Sci. Eng. **10** (2023), 1648–1658.
19. T. Dong and A. Wang, *Event-triggered consensus of nonlinear multi-agent systems with unknown external disturbance*, Asian J. Control **20** (2018), no. 5, 1928–1937.
20. X. Li, Y. Tang, and H. R. Karimi, *Consensus of multi-agent systems via fully distributed event-triggered control*, Automatica **116** (2020), 108898.
21. B. Cheng and Z. Li, *Coordinated tracking control with asynchronous edge-based event-triggered communications*, IEEE Trans. Autom. Control **64** (2019), no. 10, 4321–4328.
22. W. Xu, W. He, D. W. C. Ho, and J. Kurths, *Fully distributed observer-based consensus protocol: Adaptive dynamic event-triggered schemes*, Automatica **139** (2022), 110188.
23. C. Nowzari, E. Garcia, and J. Cortés, *Event-triggered communication and control of networked systems for multi-agent consensus*, Automatica **105** (2019), 1–27.
24. A. Girard, *Dynamic triggering mechanisms for event-triggered control*, IEEE Trans. Autom. Control **60** (2015), no. 7, 1992–1997.
25. X. Ge, Q.-L. Han, X.-M. Zhang, and D. Ding, *Dynamic event-triggered control and estimation: A survey*, Int. J. Autom. Comput. **18** (2021), no. 6, 857–886.
26. W. He, B. Xu, Q.-L. Han, and F. Qian, *Adaptive consensus control of linear multiagent systems with dynamic event-triggered strategies*, IEEE Trans. Cybern. **50** (2020), no. 7, 2996–3008.
27. Q. Hou and J. Dong, *Distributed dynamic event-triggered consensus control for multiagent systems with guaranteed performance and positive inter-event times*, IEEE Trans. Autom. Sci. Eng. **21** (2022), 746–757.
28. Q. Hou and J. Dong, *Robust adaptive event-triggered fault-tolerant consensus control of multiagent systems with a positive minimum interevent time*, IEEE Trans. Syst. Man Cybern.: Syst. **53** (2023), no. 7, 4003–4014.
29. J. Berneburg and C. Nowzari, *Distributed dynamic event-triggered coordination with a designable minimum inter-event time*, 2019 American Control Conference (ACC), 2019, pp. 1424–1429.
30. X. Wu, B. Mao, X. Wu, and J. Lu, *Dynamic event-triggered leader-follower consensus control for multiagent systems*, SIAM J. Control Optim. **60** (2022), no. 1, 189–209.
31. Z. Wang and M. Chadli, *Distributed observer-based dynamic event-triggered control of multi-agent systems with adjustable inter-event time*, 2023 62nd IEEE Conference on Decision and Control (CDC), 2023, pp. 2391–2396.
32. Z. Wang and M. Chadli, *Improved dynamic event-triggered consensus control for multi-agent systems with designable inter-event time**, 2023 31st Mediterranean Conference on Control and Automation (MED), 2023, pp. 818–823.
33. H. Zhang, G. Feng, H. Yan, and Q. Chen, *Observer-based output feedback event-triggered control for consensus of multi-agent systems*, IEEE Trans. Industr. Electron. **61** (2014), no. 9, 4885–4894.
34. J. Hu, J. Geng, and H. Zhu, *An observer-based consensus tracking control and application to event-triggered tracking*, Commun. Nonlin. Sci. Numer. Simul. **20** (2015), no. 2, 559–570.
35. X. Ruan, J. Feng, C. Xu, and J. Wang, *Observer-based dynamic event-triggered strategies for leader-following consensus of multi-agent systems with disturbances*, IEEE Trans. Netw. Sci. Eng. **7** (2020), no. 4, 3148–3158.
36. Y. Yang, D. Yue, and C. Xu, *Dynamic event-triggered leader-following consensus control of a class of linear multi-agent systems*, J. Frankl. Inst. **355** (2018), no. 15, 7706–7734 en.
37. M. Xu, M. Li, and F. Hao, *Fully distributed optimization of second-order systems with disturbances based on event-triggered control*, Asian J. Control **25** (2023), 3715–3728.
38. E. Garcia, Y. Cao, and D. W. Casbeer, *Decentralized event-triggered consensus with general linear dynamics*, Automatica **50** (2014), no. 10, 2633–2640.
39. C. A. R. Crusius and A. Trofino, *Sufficient LMI conditions for output feedback control problems*, IEEE Trans. Autom. Control **44** (1999), no. 5, 1053–1057.

AUTHOR BIOGRAPHIES

Zeyuan Wang received his B.Sc. degree in Information and Computer Science and his M.Sc. degree in System Engineering (with a minor) in aircraft design and control from Beihang University, Beijing, in 2019 and 2022, respectively, and the Engineer's Degree (the Diplôme d'Ingénieur) from CentraleSupélec, Paris-Saclay University, France, in 2022. He is currently working toward his Ph.D. degree in Control Engineering at Paris-Saclay University, France. His research interests include cooperative control and event-triggered communication of multi-agent systems, as well as topics in fault-tolerant control and distributed estimation.

Mohammed Chadli (SM'09, M'99) received his MScEng (DEA) from the Engineering School INSA-Lyon (France, 1999) and from "Ecole Normale Sup." (Mohammedia, Morocco), his PhD thesis in Automatic Control from the University of

19346093, 0, Downloaded from https://onlinelibrary.wiley.com/doi/10.1002/asjc.3385 by Universite Paris-Saclay, Wiley Online Library on [29/04/2024]. See the Terms and Conditions (https://onlinelibrary.wiley.com/terms-and-conditions) on Wiley Online Library for rules of use; OA articles are governed by the applicable Creative Commons License

Lorraine (UL), CRAN-Nancy in 2002, and his habilitation in 2011 at the University of Picardie Jules Verne (UPJV) Amiens. He was Lecturer and Assistant Professor at the "Institut National Polytechnique de Lorraine" (UL, 2000-2004). Since 2004, he was Associate Professor at the UPJV and currently Full Professor at the University Paris-Saclay, Univ Evry, IBISC Lab., France. He was a visiting professorship at the TUO-Ostrava (Czech Rep.), UiA (Norway), SMU-Shanghai (2014-2017), NUAA-Nanjing (2018, 2019) and the University of Naples Federico II (Italy, 2019).

Dr Chadli's research interests include filtering and control problems (FDI, FTC) and applications to vehicle systems, intelligence systems, network systems, and cyber-physical systems. He is an author of books and book chapters (Wiley, Springer, Hermes) of numerous articles published in international referred journals and conference proceedings and listed in "100 000 Leading Scientists in the World for career-long and single year impact.

Dr. Chadli is a senior member of IEEE. He is in the editorial board (Editor, Associate Editor) of several international journals, including the IEEE Transactions on Fuzzy Systems, Automatica, the IET Control Theory and Applications, the Franklin Institute Journal, Asian Journal of Control … and was a Guest Editor for Special Issues in international journals. He now serves as the Vice Dean of the Faculty of Sciences and Technologies (Univ Evry), and Chair of the IEEE France Section Control Systems Society Chapter.

How to cite this article: Z. Wang and M. Chadli, *Observer-based distributed dynamic event-triggered control of multi-agent systems with adjustable interevent time*, Asian J. Control. (2024), 1–13, DOI 10.1002/asjc.3385.

19346093, 0, Downloaded from https://onlinelibrary.wiley.com/doi/10.1002/asjc.3385 by Universite Paris-Saclay, Wiley Online Library on [29/04/2024]. See the Terms and Conditions (https://onlinelibrary.wiley.com/terms-and-conditions) on Wiley Online Library for rules of use; OA articles are governed by the applicable Creative Commons License